Articles

Ultratight DNA Binding of a New Bisintercalating Anthracycline Antibiotic[†]

Fenfei Leng,[‡] Waldemar Priebe,[§] and Jonathan B. Chaires*,[‡]

Department of Biochemistry, University of Mississippi Medical Center, Jackson, Mississippi 39216-4505, and The University of Texas M. D. Anderson Cancer Center, Houston, Texas 77030

Received August 21, 1997; Revised Manuscript Received November 24, 1997

ABSTRACT: Differential scanning calorimetry and absorption spectroscopy were used to characterize the interaction of the new bisintercalating anthracycline antibiotic, WP631, with DNA. The method of continuous variations revealed five distinct binding modes for WP631, corresponding to 6, 3, 1.3, 0.5, and 0.25 mol of base pairs (bp) per mole of ligand. The binding of one drug to 6 bp corresponds to the bisintercalative binding mode determined previously, and was the mode studied in detail. UV melting experiments and differential scanning calorimetry were used to measure the ultratight binding of WP631 to DNA. The binding constant for the interaction of WP631 with herring sperm DNA was determined to be 3.1 (±0.2) × 10^{11} M^{-1} at 20 °C. The large, favorable binding free energy of −15.3 kcal mol^{-1} was found to result from a large, negative enthalpic contribution of −30.2 kcal mol^{-1}. DNA melting curves at different concentrations of WP631 were fitted to McGhee's model of DNA melting in the presence of ligands, yielding an independent estimate of DNA binding parameters. The salt dependence of the WP631 binding constant was examined, yielding a slope $SK = \delta (\log K)/\delta (\log[Na^+]) = 1.63$. The observed salt dependence of the equilibrium constant, interpreted according to polyelectrolyte theory, indicates that there is a significant nonpolyelectrolyte contribution to the binding free energy. DNA melting studies using a homogeneous 214 bp DNA fragment showed that WP631 binds preferentially to the GC-rich region of the DNA.

The rational design of DNA or protein binding agents requires a thorough knowledge of the structures of related complexes along with an understanding of the thermodynamics and kinetics of complex formation. "Structure-based" design strategies have been most emphasized recently, with comparatively little attention paid to the energetic and dynamic factors that govern specific binding reactions. A comprehensive rational design strategy will incorporate knowledge of all aspects of complex formation into the formulation of principles to guide the design process. We describe here detailed thermodynamic studies of the new bisintercalating anthracycline antibiotic, WP631, whose design was based on the high-resolution structures of daunorubicin−DNA complexes (*1*, *2*). The aim of the reported studies is to study the energetics of WP631 binding in order to critically evaluate the improvement in the DNA binding properties of the bisintercalator relative to its monomeric parent compound (daunorubicin), in hopes of gaining new information to refine the design process.

The structure of WP631 is shown in Figure 1. The design strategy and synthesis of WP631 were described previously (*3*), along with experimental studies showing that it binds to DNA by bisintercalation as intended. Initial biological studies showed that WP631 could overcome a specific form of multidrug resistance in cultured cell lines, a potentially important advantage over the parent compound (*3*). High-resolution structural studies have proven that WP631 binds by bisintercalation, as intended. The structure of a WP631−$d(CGATCG)_2$ complex was determined by X-ray crystallography (*4*), which showed that the two chromophores of

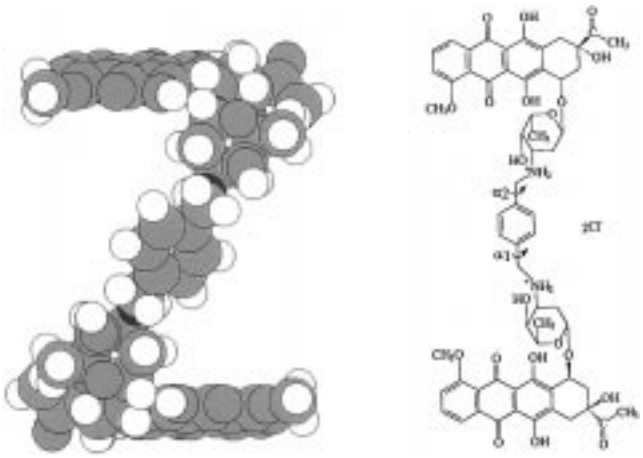

FIGURE 1: Structure of WP631. Two dihedral angles α_1 and α_2 in the linker of WP631 are shown for later reference.

[†] Supported by Grant CA35635 from the National Cancer Institute.

* To whom correspondence should be addressed at Department of Biochemistry, University of Mississippi Medical Center, 2500 N. State St., Jackson, MS 39216-4505. Telephone: (601) 984-1523. Fax: (601) 984-1501. E-mail: chaires@fiona.umsmed.edu.

[‡] University of Mississippi Medical Center.

[§] The University of Texas M. D. Anderson Cancer Center.

S0006-2960(97)02074-6 CCC: $15.00
Published on Web 01/30/1998

WP631 intercalated into the two CG steps of the DNA, with the xylene linker lining the minor groove in between. The structure of WP631 bound to $d(ACGTACGT)_2$ in solution was determined by high-resolution NMR, again demonstrating that binding was by bisintercalation (*5*).

The potential advantages of bisintercalating DNA binding agents over their monomeric counterparts have long been recognized (*6*). First, bisintercalators ought to have binding constants that are approximately the square of those of the monomers. This approximation is based on the simple additivity of binding free energies so that the free energy of bisintercalator binding is approximately the sum of two monointercalator binding free energies:

$$\Delta G_{bis} = \Delta G_{mono} + \Delta G_{mono}$$

While binding free energies are additive, binding constants are multiplicative, leading to the expectation stated above. Second, bisintercalators ought to have better binding specificity. Specificity is a direct function of site size for DNA binding agents (*7*), with larger site sizes having potentially greater absolute sequence specificity. Bisintercalators would necessarily occupy a greater number of base pairs, with potentially more stringent sequence recognition relative to the monomer. These possible advantages have motivated the rational design and synthesis of several types of bisintercalators (*6*, *8*−*10*).

Recently, the concept of dimeric analogs has been extended to protein−ligand binding reactions (*11*). For example the "SAR by NMR" strategy (*12*) is based on the same concepts outlined above, but involves the tethering of two dissimilar ligands bound to nearby sites on a protein receptor. The structure-based design of dimeric analogs emerged separately from computer modeling of ligand docking to a protein receptor (*13*). The general strategy for these protein systems is essentially the same as that which guided the earlier design and synthesis of bisintercalators, with, of course, differences in the details of the nature of the binding sites and ligands involved. A rigorous thermodynamic evaluation of the "dimeric analog" approach is of general interest and could help to refine the rational design process.

Reported here is a comprehensive calorimetric and thermal denaturation study of the ultratight binding of WP631 to DNA. The results provide an unprecedented opportunity to compare the energetics of the DNA binding of a bisintercalator and its monomeric counterpart. The expected increase in binding affinity can be critically evaluated and new information gleaned that can perhaps suggest improvements to the design process. Ultratight binding is difficult to measure accurately by traditional optical methods. The studies reported here show the utility of scanning calorimetry (*14*) and thermal denaturation with optical detection (*15*, *16*) as methods for the reliable determination of large association constants.

MATERIALS AND METHODS

Materials. The synthesis and purification of WP631 were previously described (*3*). Daunorubicin and ethidium bromide were purchased from Sigma Chemical Co. (St. Louis, MO) and were used without further purification. A molar extinction coefficient of 11 500 M^{-1} cm^{-1} at 480 nm was used to determine the concentration of daunorubicin.

Buffers. The buffers used in this work are designated as follows: BPE, 6 mM Na_2HPO_4, 2 mM NaH_2PO_4, and 1 mM Na_2EDTA, at pH 7.0; and BPES, 6 mM Na_2HPO_4, 2 mM NaH_2PO_4, 1 mM Na_2EDTA, and 185 mM NaCl at pH 7.0.

DNA Preparations. Herring sperm DNA (Boerhinger, Mannheim, Indianapolis, IN) was sonicated, phenol extracted, and purified as previously described (*17*). A molar extinction coefficient of 12 858 M^{-1} (bp) cm^{-1} at 260 nm was used for DNA concentration determinations.

A 214 bp DNA fragment (214-mer) was synthesized by amplification of the region of pBR322 between base pairs 4340 and 192, and purified as previously described (*18*, *19*). Purified 214-mer was dialyzed against BPE buffer.

Continuous Variation Analysis. Binding stoichiometries of WP631 to DNA (bp) were obtained using the method of continuous variations (*20*). The concentrations of WP631 and DNA were each varied, while the sum of their concentrations was kept constant at 50 mM (in terms of base pairs for DNA). Varying volumes of equally concentrated stock solutions of WP631 and DNA were mixed together to give a mole fraction of WP631 ranging from 0.05 to 1. The absorbance of solutions of WP631 alone was then measured at 488 nm and 24 °C, by using the same stock solution of WP631 but replacing the DNA with BPE buffer. The difference in absorbance (ΔA) was plotted against the mole fraction of drug (*20*).

UV Melting Studies. Ultraviolet DNA melting curves were determined using a Cary 3E UV/Visible Spectrophotometer (Varian, Inc., Palo Alto, CA), equipped with a thermoelectric temperature controller. Sonicated herring sperm DNA or DNA 214-mer in BPE buffer was used for melting studies. Solutions of herring sperm DNA (final concentration of 2.0×10^{-5} M bp) or 214-mer DNA (final concentration of 3.0×10^{-5} M bp) were prepared by direct mixing with aliquots from a WP631 stock solution, followed by incubation for 12 h at 24 °C to ensure equilibration. Samples were heated at a rate of 1 °C min^{-1}, while continuously monitoring the absorbance at 260 nm. Primary data were transferred to the graphics program Origin (Microcal, Inc., Northampton, MA) for plotting and analysis.

Differential Scanning Calorimetry. Differential scanning calorimetry (DSC) experiments utilized a Microcal MC2 instrument (Microcal, Inc.) along with its DA2 software (July 1986 version) for data acquisition and analysis. Sonicated herring sperm DNA at a concentration of 1 mM bp in BPE buffer was used for all experiments. A scan rate of 1° min^{-1} was used. Primary data were corrected by subtraction of a buffer−buffer baseline, normalized to the concentration of DNA base pairs, and further baseline-corrected using the Cp-(0) software option. Baseline-corrected, normalized data were transferred to the Origin graphics software package for integration and plotting. Samples for DSC of DNA and WP631 were prepared by weighing appropriate amounts of solid WP631, and dissolving the solid directly into 2 mL of a 1 mM DNA solution. Any undissolved drug was removed by low-speed centrifugation. The exact amount of WP631 bound to the DNA was then determined spectrophotometrically.

Determination of DNA Binding Constants. The DNA binding constant of WP631 was determined by DNA UV

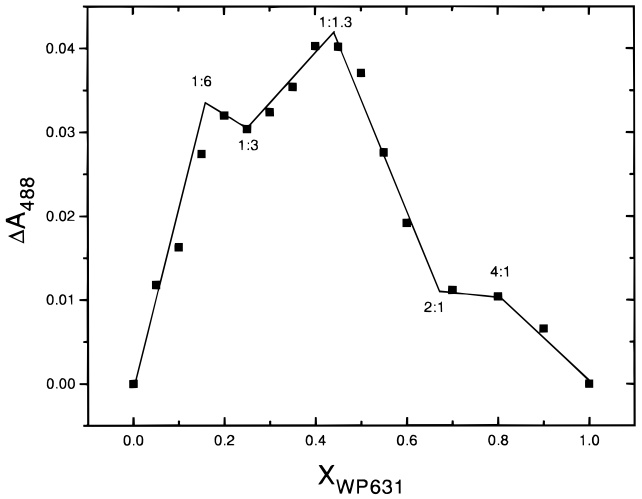

FIGURE 2: Job plot for WP631 binding to herring sperm DNA in BPE buffer. Concentrations of DNA were expressed in base pairs. The difference in absorbance (ΔA) at 488 nm as a function of the mole fraction of WP631 is shown.

melting studies. Assuming no interaction of ligand with single-stranded DNA, McGhee (*16*) derived the equation

$$1/T_m^0 - 1/T_m = (\Delta H_m/R) \ln(1+K_{T_m}L)^{1/n} \qquad (1)$$

where T_m^0 is the melting temperature of the DNA alone, T_m is the melting temperature in the presence of saturating amounts of ligand, ΔH_m is the enthalpy of DNA melting (per mole of bp), R is the gas constant, K_{T_m} is the ligand binding constant at T_m, L is the free ligand concentration (approximated at T_m by the total ligand concentration), and n is the ligand site size.

The DNA binding constant of WP631 at lower temperatures was determined by use of the van't Hoff equation:

$$\ln(K/K_{T_m}) = -(\Delta H_b/R)(1/T - 1/T_m) \qquad (2)$$

where K is the DNA binding constant of WP631 at temperature T (kelvin) and ΔH_b is the enthalpy of binding of WP631 to DNA determined by DSC.

The DNA binding constant of WP631 was also determined by analysis of complete UV melting curves at less than saturating drug concentrations, using McGhee's theory of DNA melting in the presence of ligands (*16*). A detailed description of the theory is given in the original paper (*16*). Briefly, if WP631 is assumed not to bind to single-stranded DNA, complete melting curves at a given ligand concentration may be calculated by McGhee's algorithm from the parameters T_m^0, ΔH_m, s, σ, ω_h, ΔH_b, K, and n. The parameters are defined as follows. T_m^0 is the melting temperature of the DNA in the absence of ligand. ΔH_m is the enthalpy for DNA melting in the absence of ligand. s is the equilibrium constant for forming a helix base pair from two coil nucleotides. σ is the nucleation parameter for forming a single-stranded base pair within a stretch of helix. ω_h is the cooperative parameter for ligand binding to helical base pairs. ΔH_b is the enthalpy for ligand binding to helical base pairs. K is the DNA binding constant. n is the neighbor exclusion parameter, the number of DNA base pairs in the binding site. To generate melting curves, T_m^0, ΔH_m, s, ω_h, and ΔH_b were independently determined and constrained. The parameters K, σ, and n were estimated by successive approximation. Each parameter was systematically adjusted to produce "best fit" curves that gave a minimum value of the sum of squares of residuals (SSR), the differences between observed and calculated values of melting curves, i.e., SSR $= \sum(y_{obs}-y_{calcd})^2$. In this fitting process, one parameter (K, n, or σ) was varied to construct different melting curves while all other parameters were constrained to a given value. The data derived from these calculated melting curves were used to generate SSR profiles (*25*). The plots of SSR versus these four parameters (K, n, s, and [WP631]) are shown in Figures S1−4 (Supporting Information). The minima in these plots represent the values of the parameters for the best fit of the model to the data. A FORTRAN program for calculating the DNA melting curves according to McGhee's theory was kindly provided by J. McGhee and was edited and recompiled by S. Wellman.

The DNA binding constants of WP631 at different salt concentrations were determined by DNA UV melting studies and were corrected to 20 °C by the method described above. The data were plotted as log K against log[Na^+]. The slope of this graph gives an estimate of SK of δ (log K)/δ (log-[Na^+]). This parameter can then be used to dissect the binding free energy into its polyelectrolyte and nonpolyelectrolyte components using polyelectrolyte theory (*21*).

RESULTS

Continuous Variation Analysis. Figure 2 shows the Job plot for WP631 binding to herring sperm DNA. At least five complexes with distinct stoichiometries are formed between WP631 and herring sperm DNA. The first inflection point in Figure 2 corresponds to a drug mole fraction of 0.145. This is equivalent to a stoichiometry of 6 mol of bp per mole of ligand, the stoichiometry expected for binding of WP631 by bisintercalation. The second inflection point in Figure 2 corresponds to a drug mole fraction of 0.25, which corresponds to a stoichiometry of 3 mol of bp per mole of ligand, the expected stoichiometry for monointercalation of WP631 into DNA base pairs. The third inflection point occurs at mole fraction of 0.44, which corresponds to a stoichiometry of 1.3 mol of bp per mole of ligand. The fourth and fifth inflection points occur at drug mole fractions of 0.67 and 0.80, respectively. These modes of binding correspond to 2 and 4 mol of ligand bound per mole bp. Interpretation of these multiple binding modes will be attempted in a later section. All subsequent binding studies, we emphasize, were done at mole ratios corresponding to the 1:6 (WP631:DNA bp) stoichiometry in which the drug is bisintercalated.

Determination of the DNA Binding Constant of WP631 by UV Melting Studies. Initial attempts to determine the binding constant of WP631 by traditional spectrophotometric methods failed because WP631 binds to DNA extremely tightly. UV melting studies were used to determine the binding constant for the interaction of WP631 with herring sperm DNA in BPE buffer (16 mM total Na^+). In the absence of WP631, the T_m of herring sperm DNA was found to be 67.2 °C. In the presence of 10 mM WP631, a concentration sufficient to saturate the DNA lattice, the T_m was elevated to 93.5 °C. The enthalpy of DNA melting in the absence of ligand (ΔH_m) was determined by differential

Table 1: Results from Differential Scanning Calorimetry Experiments Using Herring Sperm DNA and Complexes with WP631 or Daunorubicin[a]

	[DNA] (mM)	drug/bp	T_m (°C)	ΔH (cal/mol)
(1) HS DNA alone				
a	1.0	0	66.45	7247
b	1.0	0	66.55	7373
c	2.0	0	66.35	6854
d	8.0	0	66.65	6726
(2) HS DNA with WP631				
a	1.0	0.134	94.05	10 981
b	1.0	0.142	93.95	11 021
c	1.0	0.109	93.85	10 816
d	1.0	0.142	94.45	11 425
e	2.0	0.136	94.65	10 935
(3) HS DNA with DM				
a	1.0	0.3	100.7	12 097
b	1.0	0.33	98.7	12 096

[a] All experiments carried out in BPE buffer (16 mM total Na^+).

Table 2: Comparison of Thermodynamic Parameters for Daunorubicin and WP631 Binding to Herring Sperm DNA[a]

compound	K_{obs}	ΔG_{obs}	SK	ΔG_{pe}	ΔG_t	ΔH	ΔS
daunorubicin	1.6×10^7	−9.7	0.85	−2.0	−7.7	−10.5	−3.8
WP631	2.7×10^{11}	−15.3	1.63	−3.9	−11.4	−30.2	−51

[a] K_{obs} (M^{-1}) is the binding constant for the interaction of a ligand molecule with DNA and refers to solutions containing 0.016 M NaCl at 20 °C. ΔG_{obs} (kcal mol^{-1}) is the binding free energy calculated from the equation $\Delta G_{obs} = -RT \ln K_{obs}$. The parameter SK is the slope of the graphs shown in Figure 5. ΔG_{pe} and ΔG_t (kcal mol^{-1}) are the polyelectrolyte and the nonpolyelectrolyte contributions to the binding free energy, respectively. The polyelectrolyte contribution was calculated from the equation $\Delta G_{pe} = SK\ RT \ln[Na^+]$, evaluated at $[Na^+] = 0.0016$ M. The nonpolyelectrolyte portion of the free energy was calculated by subtraction. The enthalpy values were determined by differential scanning calorimetry. ΔS was calculated by subtraction, $\Delta S = (\Delta G - \Delta H)/T$.

scanning calorimetry to be 7.0 kcal/mol (bp), and the ligand site size (n) was determined above to be 6 bp. Equation 1 can be used with these values to determine the DNA binding constant at the melting temperature (93.5 °C), yielding $K = 8.8 \times 10^6\ M^{-1}$. For daunorubicin at 10 μM, a T_m of 87.5 °C was observed, from which a binding constant of $4.9 \times 10^5\ M^{-1}$ at the T_m may be calculated. Correction of these values to lower temperature requires knowledge of the binding enthalpy, which was determined by differential scanning calorimetry.

Table 1 shows the results of differential scanning calorimetry experiments using herring sperm DNA in the presence and absence of saturating amounts of WP631. By Hess's law, these data may be used to determine the enthalpy of WP631 binding to DNA. The equilibria to be considered, along with the experimentally determined enthalpy values, are as follows:

$$\text{duplex} \rightleftharpoons 2(\text{single strand}) \qquad \Delta H_1 = 7.0\ (\pm 0.3)\ \text{kcal mol}^{-1}$$

$$\text{WP631}-\text{duplex} \rightleftharpoons 2(\text{single strand}) + \text{WP631} \qquad \Delta H_2 = 11.4\ (\pm 1.0)\ \text{kcal mol}^{-1}$$

Combining these two reactions, the binding reaction and its enthalpy may be obtained:

$$\text{WP631}-\text{duplex} \rightleftharpoons \text{duplex} + \text{WP631} \qquad \Delta H_3 = \Delta H_2 - \Delta H_1$$

The enthalpy ΔH_3 must be corrected for the amount of WP631 bound to the DNA, and the sign changed, to obtain the binding enthalpy (ΔH_b):

$$\Delta H_b = -\Delta H_3/(\text{moles of WP631/moles of bp})$$

From five determinations, a value for ΔH_b of −30.2 (±2.6) kcal mol^{-1} was obtained for the association of WP631 with DNA. For daunorubicin, the same procedure yielded $\Delta H_b = -16.0\ (\pm 1.0)$ kcal mol^{-1}. In both cases, enthalpy values refer to the temperature at the respective T_m. [We note that the DNA binding enthalpy for daunorubicin was determined to be −10.5 kcal mol^{-1} at 20 °C by isothermal titration calorimetry (ITC) (D. Suh, F. Leng, J. Ren, and J. B. Chaires, unpublished data). The larger magnitude of ΔH_b at 99.7 °C is attributed to a small, negative heat capacity change (ΔC_p). Because of limited solubility and avid self-association, ITC cannot be used to measure ΔH_b for WP631, so we are forced to neglect any possible heat capacity changes for the binding of the bisintercalator.]

Once the binding enthalpy (ΔH_b) was determined, the DNA binding constant of WP631 at 20 °C was calculated to be $2.7 \times 10^{11}\ M^{-1}$ by application of the standard van't Hoff equation (eq 2). The same procedure was also used to determine the constant of binding between daunorubicin and herring sperm DNA, yielding a value of $1.6 \times 10^7\ M^{-1}$. Knowledge of the binding constant and binding enthalpy allowed us to construct the complete thermodynamic profiles for the binding of both WP631 and daunorubicin to herring sperm DNA. The free energy is obtained from the standard relation $\Delta G^\circ = -RT \ln K$, and the enthalpy is calculated with the equation $-T\Delta S = \Delta G - \Delta H$. The thermodynamic profiles for these two drugs are summarized in Table 2. (We note here that neglect of ΔC_p for the binding of daunorubicin in the correction of the binding constant to lower temperatures alters the estimate of the binding free energy by no more that 4%. Several practical difficulties preclude making an experimental estimate of ΔC_p for WP631. If its ΔC_p were twice as large that for daunorubicin, neglecting ΔC_p in the correction of the WP631 binding constant to lower temperatures could alter the free energy estimate by up to 15%.)

The constant for binding of WP631 to herring sperm DNA was determined independently by fitting experimental UV melting curves to McGhee's model of the helix−coil transition of DNA in the presence of ligands (*16*). WP631 was assumed not to bind to single-stranded DNA, and the following parameters were used and constrained in the fitting procedure: $\Delta H_m = 7050$ cal/mol of bp, $\Delta H_b = -30.2$ kcal/mol, $[DNA] = 5.0 \times 10^{-5}$ M bp, and $\omega_h = 1.0$. The other four parameters (n, K, s, and the effective WP631 concentration) were adjusted to produce best fit curves according to methods described in Materials and Methods. Plots of SSR versus these four parameters (K, n, s, and [WP631]) are shown in Figures S1−4 (Supporting Information) for each melting curve analyzed. The minimum in each plot represents the value of the parameter that best fits the model to the data. The experimental and the best fit melting curves are compared in Figure 3, and the resulting optimized parameters are summarized in Table 3. It should be noted

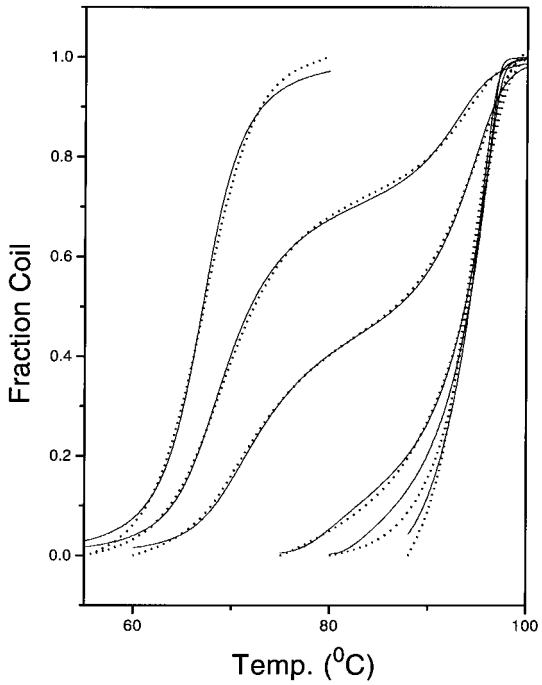

FIGURE 3: Fits of herring sperm DNA melting curves in the presence of various amounts of WP631 to McGhee's theory. The dotted lines are experimental data, and the solid lines are theoretical curves with the parameters listed in Table 3.

Table 3: Binding Parameters from Melting of Herring Sperm DNA in the Presence of WP631[a]

[DNA] (M bp)	[WP631] (M)	K (M^{-1})	n (bp)	$[WP631]_{sim}$ (M)	σ
5.0×10^{-5}	0	0	0	0	2.3×10^{-3}
5.0×10^{-5}	2.0×10^{-6}	3.3×10^{11}	6.0	1.8×10^{-6}	2.0×10^{-3}
5.0×10^{-5}	4.0×10^{-6}	3.3×10^{11}	6.0	3.6×10^{-6}	1.5×10^{-3}
5.0×10^{-5}	6.0×10^{-6}	3.0×10^{11}	6.0	6.0×10^{-6}	1.0×10^{-4}
5.0×10^{-5}	7.5×10^{-6}	2.8×10^{11}	6.0	6.5×10^{-6}	2.0×10^{-5}
5.0×10^{-5}	2.0×10^{-5}	3.3×10^{11}	6.0	7.0×10^{-6}	1.5×10^{-4}

[a] [DNA] is the concentration of herring sperm DNA. [WP631] is the total concentration of WP631 used in the experiments. K is the binding constant. n is the binding site size. $[WP631]_{sim}$ is the optimized concentration of WP631 used in the simulation. σ is the optimized nucleation parameter used in the simulation. The following parameters were constrained in the simulation: $T_m = 68.1$ °C, $\Delta H_m = -7.04$ kcal mol^{-1}, and $\Delta H_b = -30.2$ kcal mol^{-1}.

that in many cases the simulated concentration of WP631 was different from the analytical concentration used in the experiment, especially at high concentrations of WP631 (Table 3). The appropriate WP631 concentration to be used should be the free ligand concentration at the T_m. The observed differences between the analytical and optimized WP631 concentrations may originate from the strong self-association of WP631, so that the total concentration overestimates the concentration of the free monomer. Also of note in Table 3 is the fact that the nucleation parameter (σ) appeared to decrease with increasing concentrations of WP631, indicating greater cooperativity in the melting of the DNA in the presence of the drug. The analysis of five melting curves at varying WP631 concentrations yielded an estimate for K of 3.1 ($\pm$0.2) $\times 10^{11}$ M^{-1}, a value in excellent agreement with the estimate based on T_m measurements at saturating WP631 concentrations described above. Melting curves of herring sperm DNA in the presence of daunorubicin were also fit to McGhee's model (Figure 4 and Table 4).

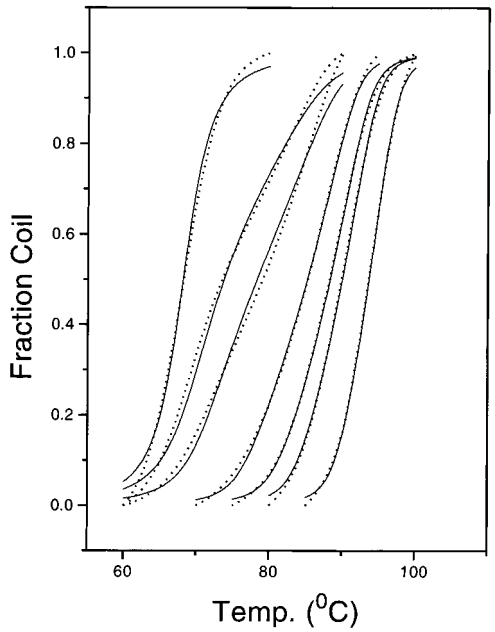

FIGURE 4: Fits of herring sperm DNA melting curves in the presence of various amounts of daunorubicin to McGhee's theory. The dotted lines are experimental data, and the solid lines are theoretical curves with the parameters listed in Table 4.

Table 4: Binding Parameters from Melting of Herring Sperm DNA in the Presence of Daunorubicin[a]

[DNA] (M bp)	[DM] (M)	K (M^{-1})	n (bp)	$[DM]_{sim}$ (M)	σ
5.0×10^{-5}	0	0	0	0	2.5×10^{-3}
5.0×10^{-5}	3.0×10^{-6}	9.2×10^{6}	3.0	3.1×10^{-6}	2.5×10^{-3}
5.0×10^{-5}	5.5×10^{-6}	9.1×10^{6}	3.0	5.2×10^{-6}	1.6×10^{-3}
5.0×10^{-5}	1.0×10^{-5}	9.2×10^{6}	3.0	9.4×10^{-6}	6.5×10^{-4}
5.0×10^{-5}	1.25×10^{-5}	9.1×10^{6}	3.0	1.25×10^{-5}	6.2×10^{-4}
5.0×10^{-5}	3.33×10^{-5}	9.2×10^{6}	3.0	2.1×10^{-5}	7.2×10^{-4}

[a] [DNA] is the concentration of herring sperm DNA. [DM] is the total concentration of daunorubicin used in the experiments. K is the binding constant. n is the binding site size. $[DM]_{sim}$ is the optimized concentration of daunorubicin used in the simulation. σ is the optimized nucleation parameter used in the simulation. The following parameters were constrained in the simulations: $T_m = 68.1$ °C, $\Delta H_m = -7.04$ kcal mol^{-1}, and $\Delta H_b = -10.5$ kcal mol^{-1}.

The resulting DNA binding constant and binding site size are also in good agreement with published values (*27*, *34*) and the values determined as described above.

Salt Dependence of the Binding Constants. UV melting experiments were used to study the salt dependence of the DNA binding of WP631. Differences between the DNA melting temperatures of DNA alone and in the presence of saturating amounts of WP631 (or daunorubicin) at different NaCl concentrations were used to calculate DNA binding constants for WP631 and daunorubicin at the melting temperature. These DNA binding constants were corrected to 20 °C by application of the standard van't Hoff equation (eq 2), assuming that the binding enthalpy is independent of salt concentration. Figure 5 shows the dependence of K at 20 °C on the concentration of Na^+ as determined by UV melting studies. The binding constants for both WP631 and daunorubicin decrease with increasing salt concentrations, due to counterion release that accompanies the binding of a charged ligand to DNA. It is possible to analyze these data

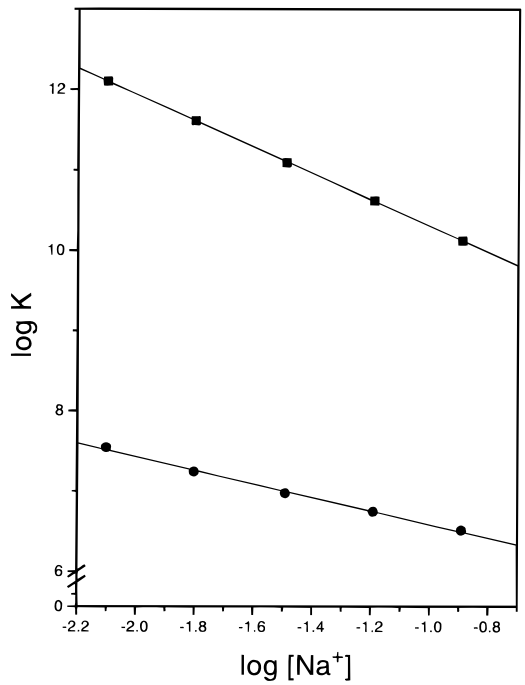

FIGURE 5: Dependence of equilibrium binding constants at 20 °C on the salt concentration for WP631 (squares) and daunorubicin (circles). Data are presented as a double-logarithmic plot according to the theory of Record et al. (*21*). The linear least-squares fits to the data are shown by the solid lines, yielding slopes of 1.63 for WP631 and 0.85 for daunorubicin.

using the polyelectrolyte theory of Record et al. (*21*). From that theory, the slopes of the lines in Figure 5 are equal to

$$\mathrm{SK} = \delta\ (\log K)/\delta\ (\log[\mathrm{Na}^+]) = -Z\psi$$

where Z is the charge on the ligands and ψ is the fraction of counterions associated with each DNA phosphate ($\psi = 0.88$ for double-stranded B-form DNA). The quantity SK is equivalent to the number of the counterions released upon binding of a ligand with net charge Z. For WP631 and daunorubicin, we found that 1.63 and 0.85 counterions, respectively, are liberated from herring sperm DNA upon binding of each ligand molecule. From these values of $Z\psi$, the charge on each ligand is as follows: +1.85 for WP631 and +0.96 for daunorubicin. These values correspond quite well to the two positive charges carried by WP631 and the one positive charge carried by daunorubicin at neutral pH.

Preferential Binding of WP631 to GC-Rich DNA. The 214 bp DNA fragment (214-mer) used in these studies has, in the absence of ligands, two sharp helix-coil transitions with T_m values of 67.3 and 71.6 °C. It was previously shown that the transition at 67.3 °C is melting of an AT-rich portion of the DNA, and that the transition at 71.6 °C is melting of a GC-rich portion of the DNA (*18*, *19*). UV melting studies of the 214-mer in the presence of increasing amounts of WP631 show unambiguously that WP631 binds preferentially to the GC-rich region of 214-mer (Figure 6). At low molar ratios of WP631 to 214-mer (0.01 and 0.025 WP631:DNA bp), WP631 has only a minor effect on the 67.3 °C transition but significantly alters the 71.6 °C transition (Figure 6). Addition of WP631 greatly increased the T_m of the 71.6 °C transition and caused this transition to become broad and biphasic. At molar ratios of 0.05 and 0.1, the GC transition became monophasic again, suggesting that the GC-rich region was saturated by WP631. The AT transition (the transition at 67.3 °C in the absence of ligands) became broad and biphasic as more WP631 was added, and its T_m was significantly increased, indicating WP631 also bound to the AT-rich region once the preferred sites within the GC-rich region were saturated. At the molar ratios of 0.2 and 0.5, both of the transitions again became sharp, indicating that both the GC-rich and the AT-rich regions were fully saturated by WP631.

DISCUSSION

These results provide a detailed thermodynamic characterization of the DNA binding of the new bisintercalating anthracycline antibiotic, WP631. WP631 is a dimeric analog of the proven anticancer drug daunorubicin. This study offers an unprecedented opportunity to compare the DNA binding energetics of a bisintercalator and its monomeric counterpart. Such a comparison is of fundamental interest and importance for the rational design process.

Binding Stoichiometry and Binding Modes. An important aim of equilibrium binding studies is to determine the binding stoichiometry of the ligand with its receptor. Binding stoichiometry is most accurately determined by the method of continuous variations (*20*, *22*, *23*). For daunorubicin, a Job plot showed only one binding mode corresponding to 3 mol of bp per mole of ligand (24; D. Suh and J. B. Chaires, unpublished data). In contrast, the Job plot of WP631 binding to DNA is complex (Figure 2). At least five distinct binding modes are evident, corresponding to 6, 3, 1.3, 0.5, and 0.25 mol of bp per mole of ligand. Multiple drug binding modes were also observed for the interaction of Hoechst 33258 with DNA (*23*), resulting in a Job plot at least as complicated as the one reported here. Plausible interpretations of the multiple WP631 binding modes are shown in Figure 7. The first mode corresponds to a 1:6 WP631:DNA bp ratio which is consistent with a bisintercalative binding mode. The crystallographic structure of the WP631−d(CGATCG)$_2$ complex was determined (*4*), where it was shown that the two chromophores of WP631 intercalated into the two CG steps of d(CGATCG)$_2$ in the complex, and that WP631 occupied 6 bp. The structure is fully consistent with the results described here. The structure of WP631 bound to d(ACGTACGT)$_2$ in solution was determined by high-resolution NMR (*5*), again demonstrating binding by bisintercalation to the central 6 bp of the oligonucleotide. The second mode in the Job plot corresponds to a 1:3 (WP631:DNA bp) stoichiometry. This stoichiometry most probably represents a monointercalation binding mode, which could arise from intercalation of a single chromophore (Figure 7C). Alternatively, a 1:3 stoichiometry could result from a more complex process in which two WP631 molecules monointercalated at nearby sites and the two remaining chromophores stacked on the outside of the DNA helix (Figure 7B). The third mode corresponds to a stoichiometry of 1:1.3 (WP631:DNA bp), which could arise from the complexes illustrated in panels D and E of Figure 7. Figure 7D shows one WP631 chromophore intercalated into DNA occupying 3 bp, while the other chromophore binds to a second WP631 molecule. This binding mode produces a binding stoichiometry of 1:1.5 drug:DNA bp ratio. The binding mode of Figure 7E shows a similar scheme, but with the intercalating chromophore

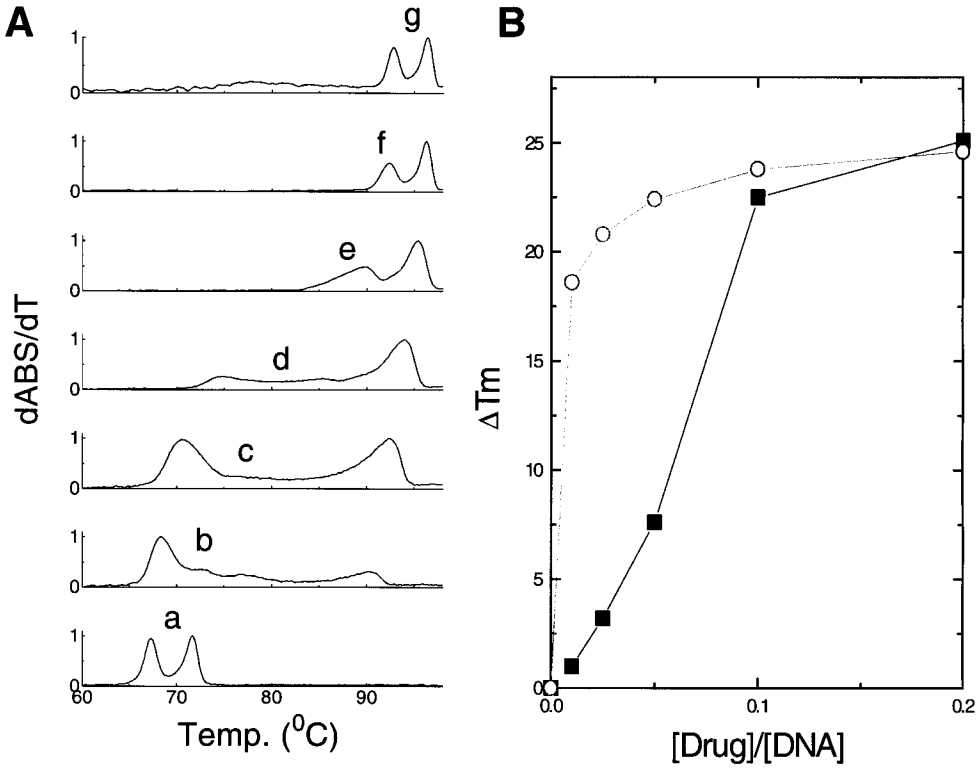

FIGURE 6: UV melting of the 214-mer in the presence of WP631 in BPE at 24 °C. The DNA concentration was 30 mM(bp). (A) Differential DNA melting curves are presented: (a) 214-mer and (b−g) WP631 and 214-mer at a molar ratio (WP631:DNA bp) of (b) 0.01, (c) 0.025, (d) 0.05, (e) 0.10, (f) 0.20, and (g) 0.50. (B) ΔT_m versus molar ratio of WP631:214-mer with open circles representing melting of the GC-rich domain and closed squares representing melting of the AT-rich domain.

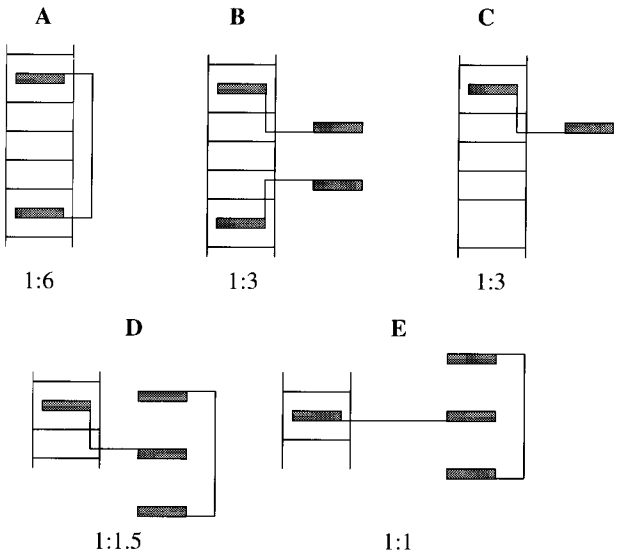

FIGURE 7: Possible binding modes for the interaction of WP631 with DNA. (A) WP631 bisintercalates into DNA and occupies 6 bp. (B and C) WP631 monointercalates into DNA and occupies 3 bp. (D) One chromophore of WP631 monointercalates into DNA base pairs and occupies 3 bp, while the other chromophore interacts with the second WP631 molecule. (E) Similar to panel D, but with 2 bp occupied by the intercalating chromophore.

occupying only 2 bp. Such a binding mode gives a binding stoichiometry of 1:1 for the ligand:DNA bp ratio. We cannot exclude either of these binding modes at this stage. The fourth and fifth modes correspond to stoichiometries of 2:1 and 4:1 (WP631:DNA bp). These are weak binding processes and appear only at high reactant concentrations. We cannot envision detailed structures for these complexes, but they could arise from drug-mediated binding processes (*23*) or from binding of aggregates of WP631 to the DNA surface. We emphasize that all subsequent thermodynamic studies were carried out under conditions that favored the primary 1:6 (WP631:DNA bp) binding mode, the bisintercalation of WP631 into DNA, that is of foremost interest.

Binding Affinity. The binding affinity of a bisintercalator for DNA ought to equal roughly the square of the binding constant of the corresponding monomer. Since daunorubicin binds to DNA with a binding constant of $\sim 10^7$ M^{-1} under the ionic conditions used here, a binding constant of $\sim 10^{14}$ M^{-1} is expected for WP631. It is very difficult to determine such a large binding constant by traditional spectrophotometric methods since it becomes impossible to work at ligand concentrations near the reciprocal of the association constant and still obtain a reliable signal. Ultratight binding may, however, be reliably studied by thermal denaturation and calorimetric methods (*14*−*16*). Therefore, we used UV melting and differential scanning calorimetry to determine the DNA binding constant of WP631, yielding a value of 2.7×10^{11} M^{-1} in BPE buffer at 20 °C. The DNA binding constant of WP631 is indeed ultratight and approaches the value expected for a bisintercalator. We emphasize that the binding constant determined by this approach necessarily represents an average value. WP631 shows a pronounced base specificity (Figure 6), and would be expected to bind to the different 6 bp binding site sequence combinations with a distribution of binding affinities. The binding constant determined by the McGhee model, which formally refers to ligand binding to an isolated site on a homogeneous lattice, would then represent a weighted average, with each site

specific association constant weighted by the frequency of each particular 6 bp sequence.

Melting curves of herring sperm DNA in the presence of increasing concentrations of WP631 were fit to McGhee's model of the helix−coil transition of DNA in the presence of ligands (*16*), making several reasonable assumptions and exploiting the opportunity to independently measure, and then constrain, several parameters. This approach provides an independent verification of the binding constant, along with a more reliable estimate of the uncertainty in the parameter estimates. The best fit curves are shown in Figure 3. To obtain these curves, we assumed that WP631 does not to bind to single-stranded DNA. T_m and ΔH_m, for the melting of herring sperm DNA, were determined independently by DSC. The DNA binding enthalpy (ΔH_b) of WP631 was determined independently by DSC. Four parameters (*K*, *n*, *s*, and [WP631]) were then left to be determined, along with some measure of their uncertainty. Plots of SSR versus these four parameters are presented in Figures S1−4 (Supporting Information); the minima in these plots correspond to the best fit values of the parameters. Table 3 summarizes the optimized parameters used to calculate the best fit curves in Figure 3. The same procedures were used to obtain optimized parameters for daunorubicin, which are summarized in Table 4, and which yielded the best fits shown in Figure 4.

The agreement between the computed curves and the data is excellent for both WP631 and daunorubicin. In particular, the shapes and biphasic behavior of the experimental melting curves (Figures 3 and 4) are matched very well by the computed curves. Notably, all of the melting curves may be matched by a single set of binding parameters for each compound The best fit produces the binding constant of 3.1 ($\pm$0.2) $\times$ 10^{11} M^{-1} and the DNA binding site size of 6 bp (Table 3). The DNA binding site size is exactly the same value we determined using the method of continuous variation and is completely consistent with the results from high-resolution structure determinations that show that WP631 occupies 6 bp (*4*, *5*). The DNA binding constant is also in good agreement with the one calculated according to eqs 1 and 2 at saturating concentrations of WP631. At low concentrations of WP631, the optimized concentrations of WP631 are almost the same as those that were used in the experiments. At high concentrations of WP631, though, the optimized concentrations of WP631 deviate from the total concentrations used in the experiments. The most likely explanation for such behavior is that it arises from the self-association of WP631 in neutral solution. The optimized concentrations of WP631 represent the effective concentrations of WP631 in the experiments and should refer to the free ligand concentrations at the T_m. Since WP631 avidly self-associates (F. Leng and J. B. Chaires, unpublished data), the concentration of active monomer would be expected to vary strongly with total WP631 concentration, exactly as the trend in the optimized concentrations suggests. The analysis of complete melting curves for daunorubicin provides estimates for the binding constant that are in excellent agreement with previously published estimates obtained more directly by fluorescence and absorbance titration methods (*27*, *34*). (We note that McGhee's method neglects any heat capacity changes for ligand binding to DNA. The excellent match between the computed and experimental curves suggests that our neglect of the small ΔC_p for daunorubicin is valid and that any heat capacity changes for WP631 can similarly be neglected without introducing too much uncertainty.)

Salt Dependence of Binding. Because WP631 is a dication, its binding to DNA is thermodynamically linked to Na^+ binding to DNA, and as a result, its DNA binding constant will depend on the total Na^+ concentration. Polyelectrolyte theories based on Manning's counterion condensation model (*21*, *26*, *27*) describe the process and provide a basis for interpreting the data of Figure 5. For WP631, the slope [δ (log *K*)/δ (log[Na+])] is found to be 1.63, which is in good agreement with the theoretical predictions by Record et al. (*21*) for dication binding to DNA. For daunorubicin, the slope is 0.85 which is in the same range as previously reported (*17*, *27*).

Dissecting the Free Energy of WP631 Binding to DNA. Knowledge of the binding constant and the binding enthalpy allows us to construct the complete thermodynamic profiles for the binding of WP631 to DNA and to begin to dissect the observed binding free energy into its component parts. From the dependence of the binding constant on salt concentration, the observed binding free energy may be partitioned into two contributions:

$$\Delta G^\circ_{obs} = -RT \ln K = \Delta G_t + \Delta G_{pe}$$

where ΔG_t is the nonpolyelectrolyte contribution to the binding free energy and ΔG_{pe} is the polyelectrolyte contribution. The latter term may be calculated from the experimentally determined quantity δ (log *K*)/δ (log[Na^+]) (=SK). Record and co-workers (*21*) have shown that ΔG_{pe} = (SK)*RT* ln[MX], where MX is the monovalent salt concentration. Table 2 summarizes the comparative energetics for the binding of daunorubicin and WP631. The magnitude of ΔG_t provides a measure of the nonpolyelectrolyte forces that stabilize the DNA−ligand complex [by "nonpolyelectrolyte" we mean all other types of molecular interactions and transfer processes other than counterion release (i.e., hydrogen bonding, van der Waals interactions, hydrophobic transfer, etc.)]. ΔG_{pe} is the free energy contribution arising from coupled polyelectrolyte effects, the most important of which is the release of the condensed counterions from the DNA helix upon binding of the charged ligand. ΔG_t for both daunorubicin and WP631 is large in magnitude, indicating that nonpolyelectrolyte forces play a significant role in stabilization of their DNA complexes. The ΔG_t value of WP631 is substantially greater than that of daunorubicin. This would be consistent with the bisintercalating binding mode by WP631 in which two chromophores have stacking interaction with the DNA base pairs, while daunorubicin only monointercalates into DNA with fewer total stacking interactions. The relative contributions to ΔG_{obs} for daunorubicin and WP631 are shown in Figure 8.

The binding enthalpy determined by differential scanning calorimetry allows the observed binding free energy to be dissected into its enthalpic and entropic components, using the standard relation $\Delta G = \Delta H - T\Delta S$. As shown in Table 2, the large, favorable binding free energy of −15.3 kcal mol^{-1} of WP631 is derived from the large negative enthalpic contribution of −30.2 kcal mol^{-1}. Binding is opposed by an unfavorable entropic contribution of $T\Delta S$ (=14.9 kcal

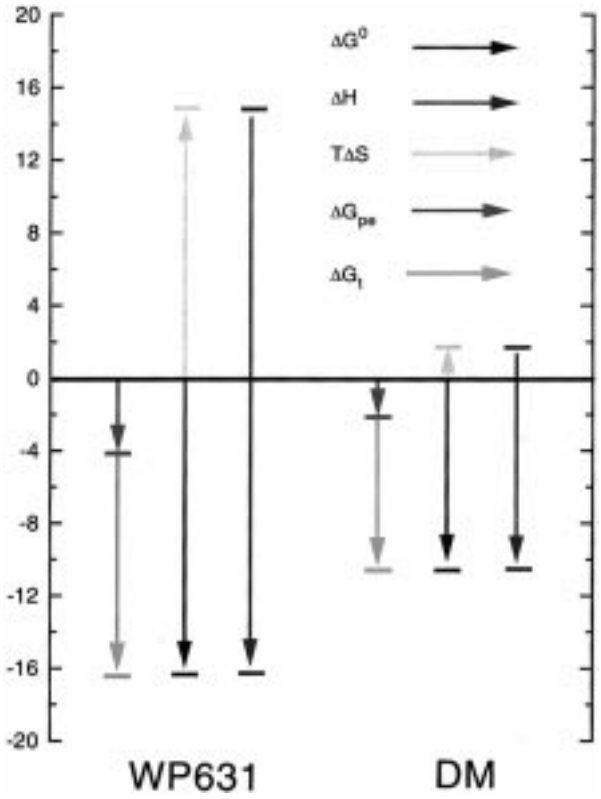

FIGURE 8: Dissection of the binding free energy ($\Delta G°$) into its polyelectrolyte (ΔG_{pe}) and nonpolyelectrolyte (ΔG_t) contributions for daunorubicin and WP631. The binding free energies and computed polyelectrolyte free energy contribution refer to solutions containing 16 mM Na^+. A comparison of the enthalpic (ΔH) and entropic ($T\Delta S$) contributions to the binding free energy of daunorubicin and WP631 is also shown. Units are kcal mol^{-1}.

mol^{-1} at 20 °C). Figure 8 summarizes the enthalpic and entropic contributions to the DNA binding free energy for WP631 and daunorubicin.

Comparison of WP631 to Daunorubicin. The thermodynamic profile for daunorubicin binding to herring sperm DNA at 20 °C is $\Delta G° = -9.7$ kcal mol^{-1}, $\Delta H = -10.5$ kcal mol^{-1}, and $\Delta S = -3.8$ cal mol^{-1} K (Table 2). Comparison shows that, while the DNA binding of both daunorubicin and WP631 is driven by the enthalpy contribution, the bisintercalator shows a substantially larger unfavorable entropic contribution. Two plausible contributions to this behavior could be: (1) the effect of WP631 on DNA structure and (2) losses of conformational freedom in WP631. The bisintercalation of WP631 could result in a proportionally larger increase of the stiffness of the DNA helix relative to daunorubicin, and thus a greater unfavorable entropic cost for the loss of DNA conformational freedom. Alternatively, the larger unfavorable entropy could come from the restriction of bond rotation. Preliminary molecular modeling studies (F. Leng and J. B. Chaires, unpublished) have indicated that there is considerable conformational freedom in WP631, with free rotation about several bonds in the linker. An unfavorable entropic contribution might come from the restriction of this conformational freedom upon bisintercalation, an effect in addition to the general entropic cost for bimolecular complex formation resulting from the loss of translational and rotational freedom of the reacting partners.

Compared to daunorubicin, WP631 has a larger favorable enthalpic contribution for the binding reaction. Its binding enthalpy is over twice the value of that observed for daunorubicin (Table 2). This larger enthalpic contribution plausibly results from the intercalation of two chromophores of WP631 into DNA, with the formation of twice the number of stabilizing molecular interactions. In addition, the xylene linker will provide new interactions in the minor groove, another possible source of favorable enthalpy.

Attribution and Additivity of Binding Free Energies. The binding of WP631 to DNA is of interest in light of the general problem of the attribution and additivity of the binding free energies of ligand substituents (*28*−*30*). The problem may be stated as follows: If a ligand molecule A−B binds to a receptor, what relationship is there between the binding energy of A−B and that of the binding energies of the separate moieties A and B? Can one assess the energetic contribution of the A and B substituents by comparing their individual binding energies with the energy of the whole molecule A−B? In general, the answer to the second question is no, and one must consider an additional term, the coupling free energy (ΔG_X). In general,

$$\Delta G_{A-B} = \Delta G_A + \Delta G_B + \Delta G_X$$

where ΔG_{A-B} is the binding free energy for the whole molecule A−B and ΔG_A and ΔG_B are the binding energies for the A and B moieties, respectively. The quantity ΔG_X is generally favorable, because of the lower entropic cost of immobilizing a single ligand rather than two (*28*). For WP631, the A and B substituents are identical, as are the daunorubicin monomers. From the data of Table 1, the coupling free energy can be evaluated:

$$\Delta G_X = \Delta G_{A-B} - \Delta G_A - \Delta G_B = -15.7 - 2(-9.7) = 3.7 \text{ kcal mol}^{-1}$$

The positive sign of ΔG_X indicates that linking two daunorubicin molecules is energetically unfavorable compared to the free energy expected from simply binding two monomers, as we discussed above. The problem now is to evaluate why. One might argue that the intercalation of one chromophore distorts the DNA to render the intercalation of the second one less favorable, by a process akin to negative cooperativity. The binding studies of Rizzo et al. (*31*) suggest that this is unlikely. In those studies, the binding of daunorubicin to a hexanucleotide was studied. Two daunorubicin monomers were bound to 6 bp, the same number of base pairs as found in the WP631 binding site. Rizzo et al. observed positive cooperativity in the binding of the second ligand, so that the binding constant for the second daunorubicin molecule was approximately 3 times higher than that for binding of the first molecule. These results contradict the argument put forth above to explain the unfavorable coupling free energy.

Another possibility was raised in the previous section, concerning the restriction of rotation around linker bonds. Knowing the magnitude of ΔG_X allows us to make a more quantitative assessment of this argument. The unfavorable free energy contribution due to the restriction of bond rotation was estimated to be $0.6N$ kcal, where N is the number of bonds whose rotational freedom is altered (*32*, *33*). The

unfavorable coupling free energy could thus arise from the restriction of 3.7/0.6 (≈6) bonds. Considering the carbon−nitrogen bond in the daunosamine along with the nitrogen−carbon and carbon−carbon bonds in the xylyl group, there are in fact six bonds in the linker that have a large degree of rotational freedom. A significant contribution to ΔG_X can be attributed to the energetic cost of the restriction of the rotational freedom of these bonds.

Other factors can also contribute to ΔG_X. A high-resolution structure of a WP631−DNA complex was reported (*4*). That structure shows that the conformations of the monomeric units in WP631 differ in subtle ways from complexes of daunorubicin alone, perhaps an additional source of unfavorable free energy. In particular, the daunosamine moieties in the WP631 complex do not fit as deeply into the minor groove as do the sugars in the complexes with daunorubicin alone (see Figure 6 in ref *4*). The distortion is such that the amine group would be placed out of range for possible hydrogen bonding interactions with the DNA bases, and van der Waals contacts of the daunosamine and the minor groove would be lessened. The energetic cost of the loss of these interactions could also make substantial contributions to ΔG_X.

Base Specificity of WP631 Binding to DNA. WP631 was designed according to the high-resolution crystallographic structures of daunorubicin−hexanucleotide complexes. Since the monomer daunorubicin preferentially binds to GC-rich DNA (*17*, *34*), WP631 was also expected to preferentially bind to GC-rich DNA. Our melting studies confirm this (Figure 6). Intercalators in general preferentially bind to GC base pairs (*35*), perhaps because of the greater polarizabilty of the GC base pair (*36*). Daunorubicin binds preferentially to the triplets 5′(A/T)CG and 5′(A/T)GC (*37*−*40*), where the notation (A/T) means that either A or T can occupy the position. WP631, which occupies 6 bp instead of 3, should have an enhanced sequence selectivity relative to that of daunorubicin. Six base pairs define the specific cleavage sites of many restriction enzymes, so the larger site size of WP631 could impart a binding specificity on par with such enzymes. In particular, WP631 would be predicted to preferentially bind to a 6 bp sequence of the type 5′GC(A/T)(A/T)GC, with intercalation of the two chromophores between the two GC dinucleotide steps, and with the linker lining the minor groove covering the two central AT base pairs. The AT base pairs would be preferred for steric reasons, since GC base pairs would introduce the N2 group into the minor groove which might hinder the fit of the linker in the groove. We note that two sequences of this exact motif may be found in the GC-rich end of the 214-mer used in our melting studies but that no such sequences can be found in the AT-rich end (*18*, *19*). The preferential binding and stabilization of WP631 to the GC-rich region could well arise from interaction at these sites. The rigorous characterization of WP631 DNA binding specificity awaits more detailed footprinting and restriction enzyme inhibition studies.

Implications for Drug Design. The rational design process requires knowledge not only of the structures of drug−receptor complexes but also of the energetics of the binding reaction. Thermodynamics can be used to shed light on the binding process and may be used to modify design strategies to improve the binding affinity. In the case at hand, the affinity of WP631 for DNA is ultratight, but its binding constant still falls short (by several orders of magnitude) of the expected value based on the affinity of monomeric daunorubicin. The thermodynamic studies described here show that the lower than expected binding free energy results from a larger unfavorable entropic contribution for WP631 relative to that for daunorubicin. From a quantitative evaluation of the coupling free energy, one plausible reason for this is due to the restriction of bond rotation in the linker. A modified design strategy in which a rigid, immobile linker was used could lead to even greater binding affinity, a specific suggestion to guide future rational design efforts. The challenge would be, however, to connect the monomeric units with such a rigid linker so that they would be in exactly the proper orientation for bisintercalation. These studies clarify that a tradeoff is made in using a flexible linker that allows an induced fit of the ligand into the binding site, but at the expense of obtaining the maximal possible binding free energy because of the energetic cost of restricting bond rotation.

Bisintercalators have been studied for well over two decades (*6*) and have been the basis for the rational design of DNA binding agents for quite some time (*8*). The dimeric analog concept has recently been extended to protein−ligand interactions, in which small molecules bound to different but nearby receptors on protein molecules are tethered together to enhance affinity (*11*−*13*). The underlying concepts and thermodynamics described in this study would be of general applicability to these newer situations involving protein binding reactions.

ACKNOWLEDGMENT

Portions of this work were submitted to the University of Mississippi Medical Center in partial fulfillment of the requirements of the Ph.D. degree (F.L.). We profusely thank Dr. Susan Wellman for providing us with a working version of McGhee's program and for her comments on the manuscript. We thank Drs. Teresa Przewloka and Izabela Fokt for their efforts in the synthesis of WP631.

SUPPORTING INFORMATION AVAILABLE

Plots of SSR versus σ, ln K, [WP631], and n (4 pages). Ordering information is given on any current masthead page.

REFERENCES

1. Quigley, G. J., Wang, A. H.-J., Ughetto, G., van der Marel, G. A., van Boom, J. H., and Rich, A. (1980) *Proc. Natl. Acad. Sci. U.S.A. 77*, 7204−7208.
2. Wang, A. H.-J., Ughetto, G., Quigley, G. J., and Rich, A. (1987) *Biochemistry 26*, 1152−1163.
3. Chaires, J. B., Leng, F., Przewloka, T., Fokt, I., Ling, Y.-H., Perez-Soler, R., and Priebe, W. (1997) *J. Med. Chem. 40*, 261−266.
4. Hu, G., Shui, X., Leng, F., Priebe, W., Chaires, J. B., and Williams, L. D. (1997) *Biochemistry 36*, 5940−5946.
5. Robison, H., Priebe, W., Chaires, J. B., and Wang, A. H.-J. (1997) *Biochemistry 36*, 8663−8670.
6. Wakelin, L. P. G. (1986) *Med. Res. Rev. 6*, 275−340.
7. Dervan, P. B. (1986) *Science 232*, 464−471.
8. Dervan, P. B., and Becker, M. M. (1978) *J. Am. Chem. Soc. 100*, 1968−1970.
9. Brownlee, R. T. C., Cacioli, P., Chandler, C. J., Phillips, D. R., Scourides, P. A., and Reiss, J. A. (1986) *J. Chem. Soc., Chem. Commun.*, 659−661.

10. Phillips, D. R., Brownlee, R. T. C., Reiss, J. A., and Scourides, P. A. (1992) *Invest. New Drugs 10*, 79−88.
11. Kessler, H. (1997) *Angew. Chem., Int. Ed. Engl. 36*, 829−831.
12. Shuker, S. B., Hajduk, P. J., Meadows, R. P., and Fesik, S. W. (1996) *Science 274*, 1531−1534.
13. Pang, Y.-P., Quiram, P., Jelacic, T., Hong, F., and Brimijoin, S. (1996) *J. Biol. Chem. 271*, 23646−23649.
14. Brandts, J. F., and Lin, L.-N. (1990) *Biochemistry 29*, 6927−6940.
15. Crothers, D. M. (1971) *Biopolymers 10*, 2147−2160.
16. McGhee, J. D. (1976) *Biopolymers 15*, 1345−1375.
17. Chaires, J. B., Dattagupta, N., and Crothers, D. M. (1982) *Biochemistry 21*, 3933−3940.
18. Falzon, L., Kink, C., Chaires, J. B., and Dabrowiak, J. C. (1994) *J. Biochem. Biophys. Methods 29*, 251−257.
19. Wellman, S. E., Sittman, D. B., and Chaires, J. B. (1994) *Biochemistry 33*, 384−388.
20. Job, P. (1928) *Ann. Chim. (Paris) 9*, 113−203.
21. Record, M. T., Anderson, C. F., and Lohman, T. M. (1978) *Q. Rev. Biophys. 11*, 103−178.
22. Cantor, C. R., and Schimmel, P. R. (1980) *Biophysical Chemistry*, pp 1135−1138, W. H. Freeman and Co., San Francisco.
23. Loontiens, F. G., Regenfuss, P., Zechel, A., Dumortier, L., and Clegg, R. M. (1990) *Biochemistry 29*, 9029−9039.
24. Walter, A. (1985) *Biomed. Biochim. Acta 44*, 1321−1327.
25. Saroff, H. A. (1989) *Anal. Biochem. 176*, 161−169.
26. Manning, G. S. (1978*) Q. Rev. Biophys. 11*, 179−246.
27. Chaires, J. B. (1996) *Anti-Cancer Drug Design 11*, 569−580.
28. Jencks, W. P. (1981) *Proc. Natl. Acad. Sci. U.S.A. 78*, 4046−4050.
29. Rappaport, H. P. (1979) *J. Theor. Biol. 79*, 157−165.
30. Crothers, D. M., and Metzger, H. (1972) *Immunochemistry 9*, 341−357.
31. Rizzo, V., Battistini, C., Vigevani, A., Sacchi, N., Razzano, G., Arcamone, F., Garbesi, A., Colonna, F. P., Capobianco, M., and Tondelli, L. (1989) *J. Mol. Recognit. 2*, 132−141.
32. Novotny, J., Bruccoleri, R. E., and Saul, F. A. (1989) *Biochemistry 28*, 4735−4749.
33. Krystek, S., Stouch, T., and Novotny, J. (1993) *J. Mol. Biol. 234*, 661−679.
34. Chaires, J. B. (1990) *Biophys. Chem. 35*, 191−202.
35. Wilson, W. D. (1990) in *Nucleic Acids in Chemistry and Biology*, (Blackburn, G. M., and Gait, M. J., Eds.) pp 297−336, CIRL Press, Oxford.
36. Muller, W., and Crothers, D. M. (1975) *Eur. J. Biochem. 54*, 267−277.
37. Chaires, J. B., Fox, K. R., Herrera, J. E., Britt, M., and Waring, M. J. (1987) *Biochemistry 26*, 8226−8236.
38. Chaires, J. B., Herrera, J. E., and Waring, M. J. (1990) *Biochemistry 29*, 6145−6153.
39. Chen, K.-X., Gresh, N., and Pullman, B. (1987) *J. Biomol. Struct. Dyn. 3*, 445−466.
40. Pullman, B. (1991) *Anti-Cancer Drug Des. 6*, 95−105.

BI9720742